FATIGUE CRACK GROWTH IN AUSTENITIC STAINLESS STEEL PIPING

M. Bethmont [*], J.L.Cheissoux [**] and J. Lebey [***]

[*] Framatome, Tour Fiat, Cedex 16, F 92084 Paris, La Défense - France

[**] CEA - Centre d'Etudes Nucléaires de Cadarache B.P. N°1 F 13115 Saint Paul lez Durance-France

[***] CEA-Centre d'Etudes Nucléaires de Saclay B.P. N°2 F 91190 Gif sur Yvette-France

INTRODUCTION

The study presented in this paper is being carried out with a view to substantiating the calculations of the fatigue crack growth in pipes made of 316 L stainless steel. It is undertaken jointly by FRAMATOME and the CEA so that the results obtained may be applied to P.W.R. primary piping. It is divided into two parts. First, fatigue tests (cyclic pressure) are carried out under hot and cold conditions with straight pipes machined with notches of various dimensions. The crack propagation and the fatigue crack growth rate are measured here. Second, calculations are made in order to interpret experimental results. From elastic calculations the stress intensity factor is assessed to predict the crack growth rate. The results obtained until now and presented in this paper relate to longitudinal notches.

DESCRIPTION OF TESTS

Cyclic variations of stress required to propagate the defects are obtained with cyclic variations of internal water pressure on experimental pipes either at room temperature or at P.W.R. temperature ($\sim$ 300°C).

Test Equipment

For tests at room temperature, a special device including a pump and a set of electro-valves is used; on this device, maximum and minimum pressures are adjustable and the frequency of cycles is about 4 cycles per minute. Hot condition tests are carried out on the "Aquitaine 1" pressurized water loop, which operates at P = 160 bars and T = 285°C. On this loop a derivated circuit including the test pipe can be periodically isolated from the main circuit by means of two electro-valves. After maintaining the test section a few minutes under a pressure of 160 bars, the pressure is dropped to three bars by opening a third electro-valve connected to a condenser. After re-injecting the condensed water into the main circuit, a new cycle can be started. The operating frequency for these tests is 4 cycles per hour, and the temperature of the test pipes is 285°C. More details are given by Doyen and co-workers (1977) and Bethmont and co-workers (1979).

Test Pipes

The dimensions of the test pipes, at a scale of 0.25 of straight parts of primary piping of P.W.R. reactors, are :

O.D. 219.5 mm I.D. 185.5 mm Thickness 17 mm

The lengths are 650 mm for the pipe n°1 and 1500 mm for the others. All the pipes were tested with longitudinal external or internal machined notches with an initial depth a_o equal to 0.5 times the wall thickness (i.e. 8.5 mm). The total notch lengths 2c are specified on table 1.

Material

The tensile characteristics of the stainless steel 316 L of the test pipes are as followed :

t° (degres C)	$\sigma_{y\ o,2\%}$ (MPa)	$\sigma_{u.T.S}$ (MPa)
20	233	558
285	167	457

The fatigue crack propagation curves $da/dN = f(\Delta K_I)$ were determined by three different laboratories for various conditions of environment, temperature and frequency. The tests were carried out on CT specimens made of 316 L taken from pipes or sheets (Doyen 1976 and Bernard 1977). Test conditions and results are set forth on table 2. ΔK_o and n represent the values of the constants of the crack propagation law expressed as following :

$$da/dN = 10^{-4}\ (\Delta K/\Delta K_o)^n$$

Experimental Program

As will be demonstrated in what follows, only a rather limited program at elevated temperature was carried out. This is due to the numerous loop troubles which arise during working. As a consequence, most of the tests were carried out at room temperature by means of the above-mentioned special device. When hot condition tests were possible, crack initiation was obtained by cold pressure cycles before mounting the test pipes on the loop in order to reduce the number of valve operations. Test conditions of the five experimented notches are summarized on table 1.

Crack Growth Measurements

A preliminary attempt to measure crack propagation by the ultrasonic method was made, but the results were not seemed reliable. After tests, crack growth was measured by micrographic examinations (inter-striae measurements). From these measurements it was possible to determine the crack growth rate and the crack depth versus number of cycles.

EVALUATION OF STRESS INTENSITY FACTOR

Several methods for determining the stress intensity factor K_I, along the crack front, have been used : - 3-D finite element calculations,
- values given by Heliot, based on his own analysis,
- ASME code evaluations.

Three-dimensional finite element calculations : BILBO code of CASTEM system (Charras 1978) was used to carry out the 3-D elastic calculations. Twenty noded (cubic) and fifteen noded (prismatic) isoparametric elements were employed.

Three studies were made of three cracks of differing dimensions (see table 3). Three types of loadings act in every case on the two faces of the cracks : uniform, linear and parabolical pressure. Due to the symmetry of the geometry involved in the problem, only one quarter of the pipes was analysed. Finite element calculations give numerical values of stress and displacements at each point of the mesh. The analytical expression of the elastic singular solution corresponding to the plane strain is :

$$u = (2(1-\nu^2)/E)K_I\ \sqrt{2r/\pi}$$

with u = normal displacement
E,ν = elastic constants
r = distance from the crack front

K_I values are deduced all along the crack front on the basis of the expression :

$$K_I = \lim_{r \to o}\ (E.u/2(1-\nu^2))\ \sqrt{\pi/2r}$$

In order to obtain accurate results with this method a refined mesh is required near the crack front. The mesh involves a large number of elements and great cost of calculation. For example, the mesh is composed of 1897 nodes and 340 elements for the longest crack. When the crack border intersects with a free surface, the above formulas corresponding to plane strain can no longer be used. Accurate values of K_I at this point of intersection cannot be obtained, especially when the angle at which the crack intersects with the boundary is other than 90°. Results obtained are presented on figure 1. The shape factor F is plotted against a position on the crack front s/so for an uniform pressure acting on the two faces of the crack. F variations along the crack front are small except for the longest crack (2c = 170 mm). It is to be noted that F at the central point of this longest crack is almost the same as that obtained from a 2-D analysis, assuming an infinite crack length. In case F = 2,28 (Heliot, 1977).

Heliot's Conclusions

Heliot analysed semi-elliptical surface flaws for various ratios a/t and a/c on plates and cylinders for which Ri/t = 10 (pressure vessel geometry). He used the weight function method and boundary integral equation calculations (Heliot and co-workers, 1979 a, 1979 b). His conclusions relating to the F factor at the central point of the flaw are summarized on table 3. The differences between his results and 3-D finite element values can be attributed to the various flaw shapes and thicknesses analysed.

ASME Code Evaluations

The ASME code (1979) sets forth a simple method for determining K_I using the membrane and bending stresses at the location of the flaw :

$$K_I = (\sigma_m M_m + \sigma_b M_b)\ \sqrt{\pi\ a/Q}$$

M_m, M_b and Q have been plotted in figures versus ratios a/c and a/t at the control point of the flaw. Results for the membrane stress are presented in table 3. Slighthy conservative values of F are obtained by this assessment method.

Factor F assessments for Various Crack Depths

Until now, values of F were determined for initial flaw dimensions. To analyse the crack growth, it is necessary to assess F in accordance with increasing flaw depths. Such values are given by Heliot (1979 b) and summarized in table 4. On this basis, the stress intensity factor range ΔK can be calculated for such fatigue crack growth assessments as :

$$\Delta K = K_{max} - K_{mini}$$

$$= F\ (a/_t\ ;\ a/_c)\ \Delta\sigma\ \sqrt{\pi a}$$

where $\Delta\sigma$ is the hoop stress range during a cycle. For internal flaws, pressure which acts directly on crack faces must be added to $\Delta\sigma$.

EXPERIMENTAL RESULTS AND COMPARISON WITH PREDICTIONS

The first stage of the analysis involves comparing the (da/dN, ΔK) results from C.T. specimens with the experimental (i, ΔK) results in pipes. da/dN is the macroscopic crack growth rate measured on the sides of the C.T. specimens and i is the interstriae-measurements on surfaces of the cracks in pipes. Results obtained at 20°C in air or water environment are presented on fig. 2. These results correspond to the crack growth rate at the center of the crack front where the stress intensity factor reaches its maximum value. There is a correspondance to be observed between predictable da/dN from the reference curves and the measured values on pipes, except for two points relative to pipe 4, which was subjected alternatively to cyclic variations of pressure at 20°C and 285°C (see table 1). ΔK values for pipe 1 result from two modes of calculations of $\Delta\sigma$. First $\Delta\sigma$ expressed in a polynomial form :

$$\Delta\sigma = \Delta\sigma_0 + \Delta\sigma_1 (x/t) + \Delta\sigma_2 (x/t)^2$$

(see open points on fig. 2)
Second, $\Delta\sigma$ is approximated to $\Delta P\ (R_i/t)$ (black points on fig. 2). This latter method provides an over-estimation of ΔK and can be used with a high degree of reliability for calculations. For the few results obtained in hot conditions a larger discripancy can be observed (fig. 3). Only two points of measurement are in agreement with the C.T. results. The interstriae-measurements of the internal crack (in water environment) are larger than expected. An experimental study has been carried out to determine a correlation between da/dN and i on the C.T. specimens. A similar study has already been made on 304 stainless steel (Hadida and Sama Itoua 1976). Its results show that differences between da/dN and i depend on ΔK.
An example of crack propagation calculation is given on fig. 4 in comparison with the measured crack growth versus number of cycles obtained from the counting of number of striae. Fig.4 sets forth the growth of the internal crack of pipe 4 at 20°C. The experimental results are found inside the scatter band deriving from calculations carried out according to the various propagation laws given in table 2.

REFERENCES

ASME Code (1979) section XI. Appendix A

Bernard, J.L., and others (1977). Validation des caractéristiques de calcul des matériaux constituant le circuit primaire des réacteurs P.W.R. Presented at Int. Symposium on Appl. of Reliability Tech. to Nuclear Power Plants (Vienna)

Bethmont, M., J.J. Doyen and J. Lebey (1979). Crack growth rate of P.W.R. piping. Presented at the 5th SMIRT Conference (Berlin).

Charras, T (1978), Système CEA-SEMT. Programme BILBO. Notice d'utilisation. Rapport CEA N°1936

Doyen, J.J. (1976). Boucle Aquitaine. Synthèse des Essais Metallurgiques. Rapport Framatome. DT/D 76-118

Doyen, J.J., J. Lebey, and M. Vrillon (1977). Crack Growth Rate Analysis in P.W.R. Reactor piping. Presented at the 4th SMIRT Conference (San Francisco).

Hadida, A., and Sama-Itoua (1976). Etudes des mécanismes de fissuration en fatigue-corrosion dans l'eau salée de l'acier inoxydable austénitique type Z6 CND 17-12 (AISI 316). Thèse Université de Technologie de Compiègne.

Héliot J., R.C. Labbens and A. Pellissier-Tanon (1979a). Semi-elliptical cracks in a cylinder subjected to stress gradients - Fracture Mechanics, ASTM - STP 667, p.p. 341-364.

Héliot J., (1979b). Fissures semi-elliptiques axiales de grande largeur (a/c = 1/10) débouchant à l'intérieur d'un cylindre (t/R_i = 0,1). Calcul de la répartition des facteurs d'intensité de contrainte le long du contour. Rapport Creusot Loire NT 79/28.

Héliot J. (1977). Fissure axiale extérieure dans un cylindre R_i/W = 5. Calcul de K à partir d'une approximation polynomiale des contraintes. Rapport Creusot Loire 423.

TABLE 1. Description of tests

PIPE N°	NOTCH	START OF TESTS → CONDITIONS OF TESTING → END OF TESTS						OBSERVATIONS
1	INFINITE EXTERNAL	5880 Cycles at T = 20°C ΔP = 162 bars						LEAK AT CRACK
2	INTERNAL 2c = 170	6480 Cycles at T = 20°C ΔP = 197 bars						LEAK AT CRACK
	EXTERNAL 2c = 340	1910 Cycles at T = 20°C ΔP = 197 bars						LEAK AT CRACK
4	INTERNAL 2c = 50	6000 cycles at T=20°C ΔP=197 bars	1650 cycles at T=285°C ΔP=157 bars	62,500 cycles at T=20°C ΔP=197 bars	← End of internal crack testing			LEAK AT INTERNAL CRACK
	EXTERNAL 2c = 50				5000 cycles T=20°C ΔP=197 bars	5350 cycles T=285°C ΔP=157 bars	16,670 cycles T=20°C ΔP=197 bars	NO LEAK

TABLE 2. Tests on CT specimens

Environment	PARAMETERS OF TESTS t° Degres C	R	Frequency	CONSTANTS ΔKo (Mpa√m)	n	CASE N°	LABORATORY	SEE REFERENCE
AIR	20°	0	20 Hz	31,3	4,4	①	A	(1)
		0.09	35 Hz	26,5	5	②	B	(1)
		0.02	10 Hz	25,7	4,17	③	A	Unpublished
		0.3	100 Hz	27	4,2	④	C	(1)
	320°	0	10 Hz	22,6	4,9	⑤	A	(1)
		0.02	10 Hz	23,7	5,33	⑥	A	Unpublished
PWR WATER 155 BARS	320°	0	4 cycles/min.	20	2,73	⑦	A	(2)
		0	4 cycles/hour	17	3,82	⑧	A	(2)

(1) : Doyen (1976)
(2) : Bernard (1977)

TABLE 3. Shape factor for initial geometry at the deepest point of the flaw (point A).

$$F = \frac{K_I}{\sigma \sqrt{\pi a}}$$

PIPE	LOCATION OF FLAW	a/t	a/c	SHAPE FACTOR : F		
				FINITE ELEMENTS (BILBO)	AFTER HELIOT	ASME (Section XI)
1	External	0.50	0.	-	2.22	-
2	External	0.53	0.05	-	2.10	-
	Internal	0.55	0.10	2.12	1.64	2.26
4	External	0.50	0.33	1.28	1.17	1.33
	Internal	0.50	0.34	1.22	1.17	1.32

TABLE 4. Values of F after Heliot for various amounts of crack growth (at point A).

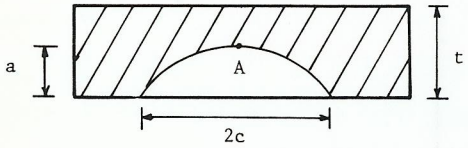

PIPE 1 external crack 2c = ∞		PIPE 2 external crack 2c = 340		PIPE 2 internal crack 2c = 170		PIPE 4 external crack 2c = 51		PIPE 4 internal crack 2c = 50	
a/t	F	a/t	F	a/t	F	a/t	F	a/t	F
0,54	2,48	0,53	2,10	0,55	1,64	0,50	1,17	0,5	1,17
0,615	2,94	0,60	2,32	0,60	1,75	0,61	1,18	0,60	1,18
0,685	3,45								
		0,70	2,62	0,70	1,90	-	-	0,70	1,12
0,75	3,96							0,75	
		0,78	2,88						
0,807	4,45			0,80	1,95	-	-	0,80	1,07
0,860	4,87	-	-	0,98		-	-	0,90	∿ 1,00

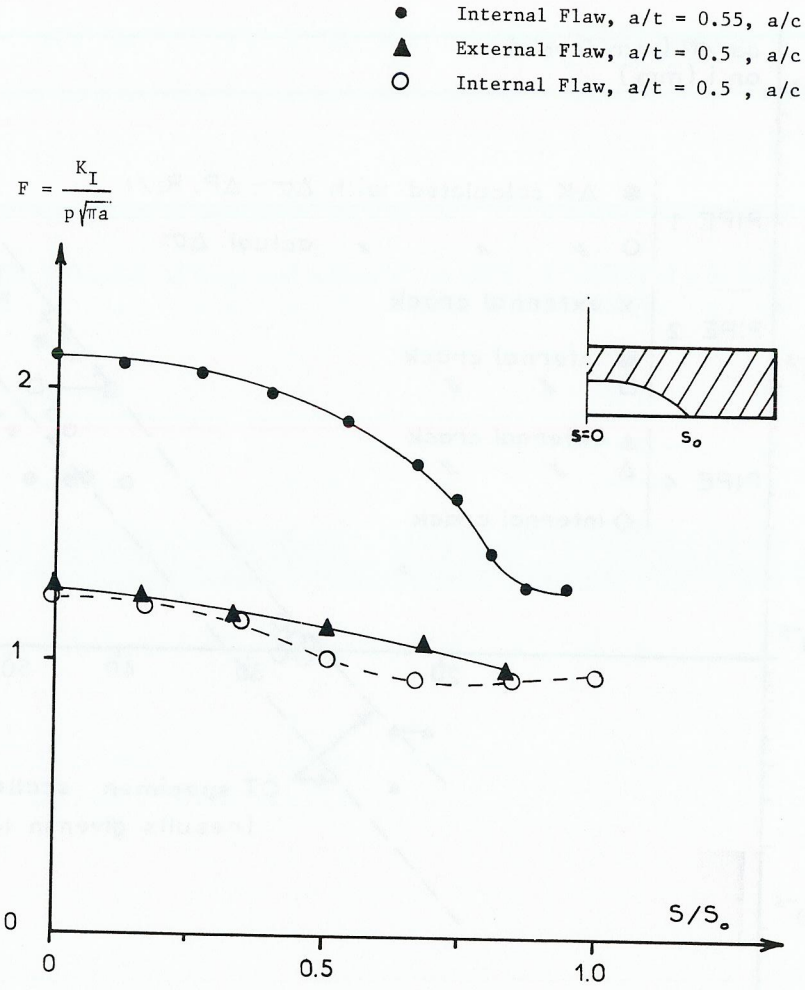

Fig. 1. Variation of shape factor along the crack front (3-D F.E calculations)

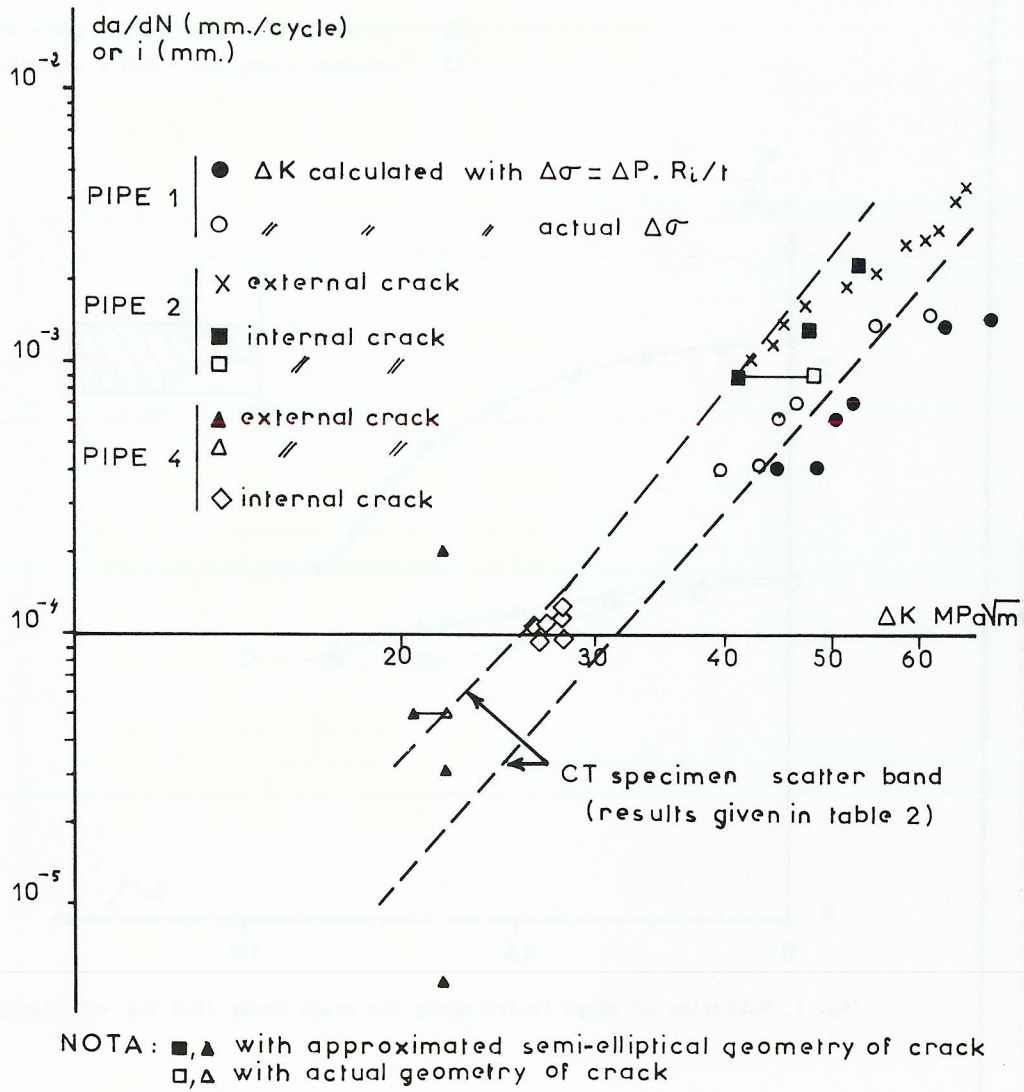

Fig. 2 Fatigue crack growth on CT specimens and pipes at 20°C

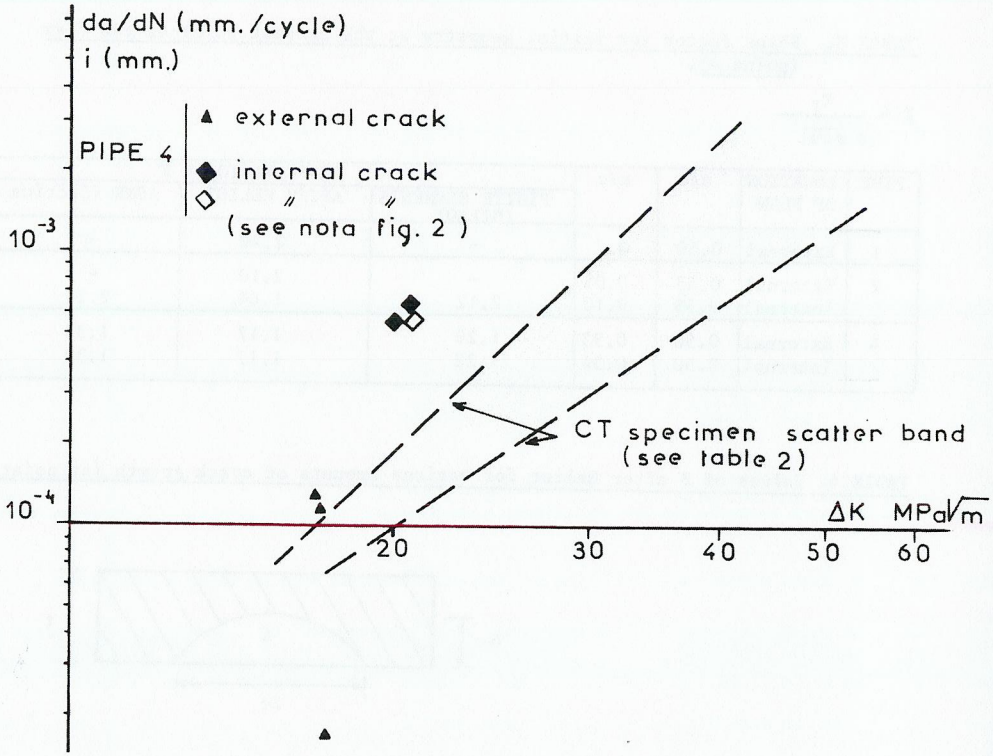

Fig. 3 Fatigue crack growth on CT specimens and pipes at 285°C

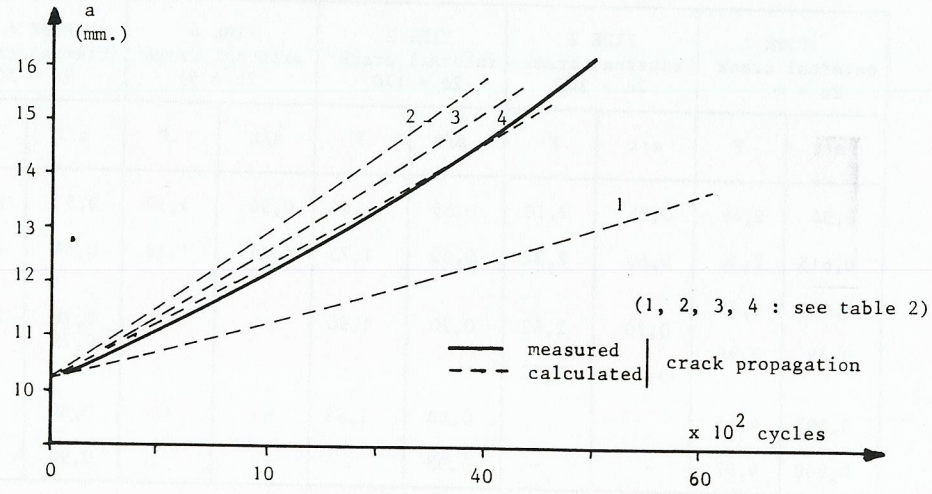

Fig. 3 Measured and expected crack propagation on pipe 4